

SYNTHESIS, STRUCTURAL AND SURFACE MORPHOLOGICAL CHARACTERIZATIONS OF SULFATED ZIRCONIA NANOPARTICLES VIA CHEMICAL ROUTE

B. A. Ezekoye^{1,*}, F. I. Ezema², V. A. Ezekoye³, P.O. Offor⁴, U. Uduh⁵

^{1,2,3,5}DEPARTMENT OF PHYSICS AND ASTRONOMY, UNIVERSITY OF NIGERIA, NSUKKA, NIGERIA.

⁴DEPARTMENT OF METALLURGICAL AND MATERIALS ENGINEERING, UNIVERSITY OF NIGERIA, NSUKKA, NIGERIA

E-mail addresses: ¹ benjamin.ezekoye@unn.ed.ng, ² fiezema@yahoo.com; ³ vaezekoye@yahoo.com; ⁴ peterjoyoffor@yahoo.com; ⁵ uduchristiana@gmail.com

Abstract

Sulfated zirconia (SZ) nanoparticles (NPs) were successfully synthesized and deposited via chemical route called sol-gel technique. The structural, morphological, and optical properties the samples were investigated by X-ray diffraction (XRD), Energy Dispersive X-ray Spectrometry (EDX), Scanning Electron Microscopy (SEM) and UV-visible spectrophotometer. Results show that the transmittance of the samples increased from visible region (VIS) to infrared (UV) region. It also showed that the transmittance of the samples changed with the precursor's concentrations. Furthermore, the samples showed very low absorbance which decreased toward the infrared region. The nanoparticles have wide energy bandgap that varied from 3.80 to 4.00±0.05 eV and is therefore good candidate for solar cell and solar thermal applications. It also presents an attractive alternative material for biomedical implants due to its biocompatibility and mechanical strength.

Keywords: Sulfated zirconia, sol-gel, nanoparticles, X-ray diffraction, wide-bandgap

1. Introduction

Sulfated Zirconia (SZ) has interesting mechanical, thermal and physicochemical properties such as high hardness, good shock and wear resistance, strong acid and alkali resistance, low frictional resistance, and high melting temperature [1-2]. The tetragonal-to-monoclinic martensitic phase transformation has serious technological implications as it helps in the toughening of ceramics (ceramic steel), and has attracted much attention of researchers in the recent years [3, 4]. It is used in preparing piezoelectric (PZT) ceramics which have been widely used due to its superior performance and it can also be used to fabricate oxygen sensors. Furthermore, sulfated zirconia is a well-known solid acid catalyst [5, 6], and has shown potential applications at ambient temperature. These promising properties of sulfated zirconia can therefore be utilized as an abrasive, as a hard, resistant coating for implants and cutting tools, in high temperature engine components and as a structural and functional material [7, 8, 9, 10]. Zirconia nanoparticles are

also of great interest due to their improved optical and electronic properties with application as electro-optic and dielectric materials [8-10]. Furthermore, Zirconia is also being recently used as solid acid catalyst [11].

The synthesis of sulfated zirconia has been realized by physico-chemical methods such as sol-gel synthesis [12] [17], aqueous precipitation [13], thermal decomposition [14], spray pyrolysis [18, 19, 20, 21] and hydrothermal synthesis [15]. Also the possibility of doping the particles has been studied [19]. However, all these methods require extremes of temperature (in the case of thermal synthesis) and pressure (hydrothermal synthesis). Rapid solid-state metathesis reactions [16] are also used successfully but have some limitations in applications due to the high cost and high temperature. Biological methods for material synthesis would help circumvent many of the above detrimental features by enabling synthesis at mild pH, pressure and temperature and at a substantially lower cost [1, 7]. Depending on the method different production

* Corresponding author, Tel: +234-8037786767

rates and particle size ranges can be covered. Most often utilization of the method is linked with the type of precursor. Usually in spray pyrolysis, precursor salts such as $Zr(NO_3)_2$ [21], dissolved in a sprayed liquid, are used with final particle size given predominantly by the precursor concentration. Gas phase pyrolysis uses thermal decomposition of vaporized precursors such as organometallic compounds [19] or chlorides [20]. The nanoparticles can be prepared through using various novel and enhanced deposition techniques such as sol-gel technique which has the advantage that sol-gel sample can be produced in different forms such as bulks, thin films and particles.

In the present work sulfated ZrO_2 nanoparticles was synthesized by simple and economical sol-gel technique using varying precursor concentrations. The synthesized sulfated zirconia (SZ) nanoparticles (NPs) were further characterized for structural, surface morphological and optical properties by X-ray diffraction (XRD), Energy Dispersive X-ray Spectrometry (EDX), Scanning Electron Microscopy (SEM) and UV-VIS spectrophotometry.

2. Experimental Details

2.1. Materials:

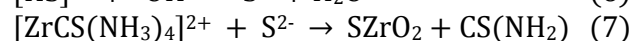
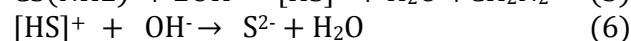
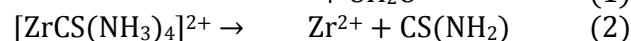
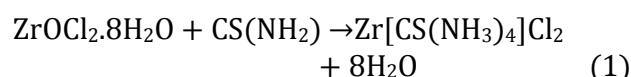
The precursors (chemicals) for the preparation of Sulfated zirconia nanoparticles are zirconium oxychloride ($ZrOCl_2 \cdot 8H_2O$), thiourea ($CS(NH_2)_2$), and distilled water. The chemicals were used as procured without further purification.

2.2. Methods:

The precursors were first dispersed with a solvent to form starting solution, a low viscosity solution called sol. Stepwise addition of the elements with constant stirring resulted in homogenous solution which was heated for 30 minutes to about 373 K to form a gel. The precursors of three different concentrations

reaction baths were prepared for samples M1, M2 and M3. Prepared glass substrates were vertically inserted into the bath solution for 1hr to deposit thin films. After the gel like solution was then filtered, washed with distilled water and dried in the oven for 2hours 30minuites to obtain nanoparticles. The resulting nanoparticles were further calcined (annealed) at temperature of 573K for 1hour to obtain solid sulphated zirconia (SZ) nanoparticles. The structural, morphological, and optical properties the samples were examined by X-ray diffraction (XRD) (PANalytical: anode material: CuK-alpha of wavelength 1.540601[Å], generator settings: 40.00 mA, 45.00 kV, 25.0°C), energy dispersive X-ray Spectrometry (EDX) operated at 14.00 KeV, Scanning Electron Microscopy (SEM) operated at 20.00 kV and UV-VIS spectrophotometer machine, PYE-UNICAM UV-2102 PC (350-1000 wavelength).

The suggested chemical reaction to produce sulphated zirconia (SZ) is as follows:



3. Results and discussions

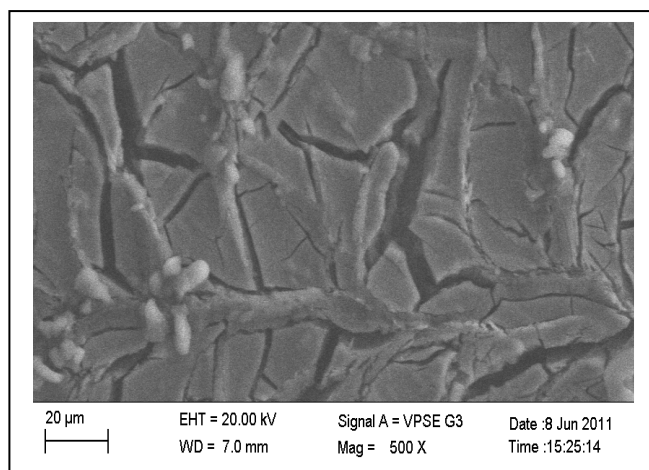
The following results were obtained from the characterizations of Sulphated zirconia (SZ) nanoparticles prepared using sol-gel technique.

3.1. SEM Study

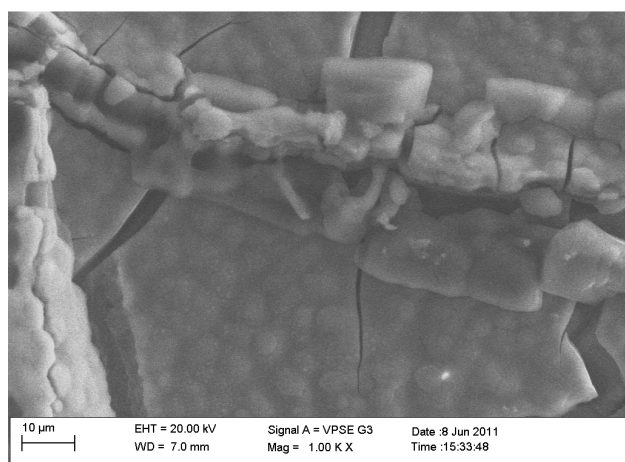
Fig. 1 shows the scanning electron micrograph (SEM) of the film carried out at operating voltage of 20 kV. The micrograph with magnification (5Kx) reveals nanoparticles.

Table 1 Compositions of precursors for preparation of sulphated zirconia (SZ).

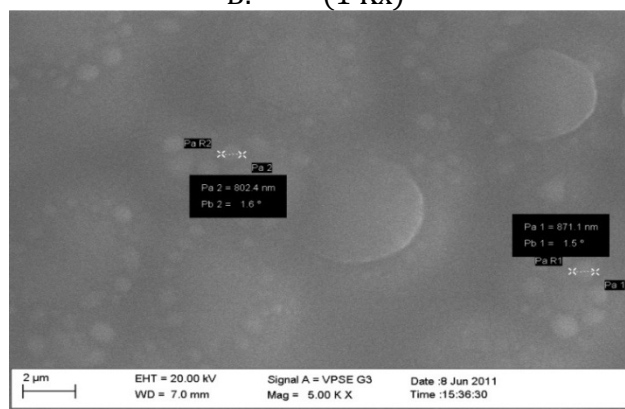
Reaction/Sample	$ZrOCl_2 \cdot 8H_2O$		$CS(NH_2)_2$		$H_2C_2O_4$		H_2O Vol (ml)
	Mol(M)	Mass(g)	Mol(M)	Mass(g)	Mol(M)	Mass(g)	
M3	0.5	4.83	1.0	2.28	0.5	1.35	30.0
M1	1.0	9.67	1.0	2.28	1.0	2.70	30.0
M2	0.5	4.83	0.5	1.14	1.0	2.70	30.0



A. (.5 Kx)



B. (1 Kx)

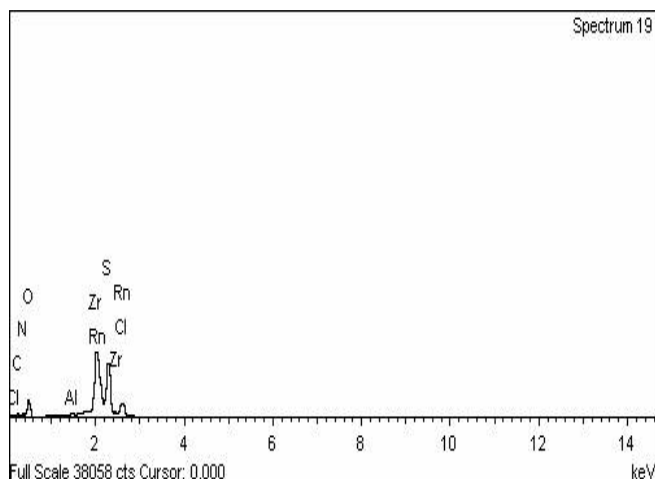


C. (5 Kx)

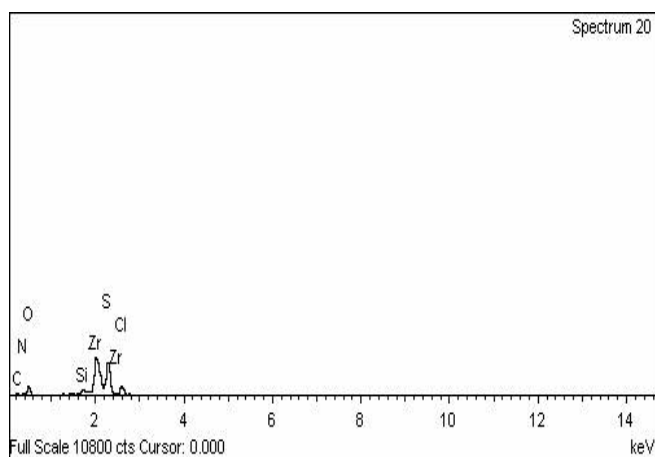
Fig. 1: SEM images of sulphate zirconia (SZ) for thin films (A) x500, (B) x1000 and (C) x5000 nanoparticle samples.

3.2. Energy Dispersive X-ray Spectrometry (EDX)

Fig. 2 shows the Energy Dispersive X-ray Spectrometry (EDX) of the sulphated zirconia (SZ) film carried out at 14KeV revealed the elemental composition of sulphated zirconia (SZ) with empirical ratios: 0.14: 0.27:0.25 ($S_{0.14}/Zr_{0.27}O_{0.25}$).



A



B

Fig. 2: EDX spectra of for Sulphated zirconia (S/ZrO_2) sample M3

3.3. X-Ray Diffraction (XRD) Stud

The XRD patterns of deposited M3 samples of sulphated zirconia (SZ) are shown in Fig. 3 and reveal the peak related value of the diffraction at 2θ between 20° and 80° and peak related values of 23.15° and 26.89° for deposited precursor materials respectively.

I. Crystalline structure of the film: from XRD result the film was found to have tetragonal crystalline structure.

II. Preferred orientation (Miller indices): The preferred orientations of the film at the peak values of the diffraction are (200) and (021) for M2 and M3 samples respectively.

III. Crystalline size, D: The crystalline size of the film can be calculated using the famous Debye-Scherrer's relation [7]:

$$D = \frac{0.9\lambda}{\beta \cos \theta} \quad (8)$$

where $\lambda = 1.5406 \text{ \AA}$ is the wavelength of CuK_{α} , $\beta = 0.010$ rad, which is full width at half maximum (FWHM) and $\theta =$ Bragg angle, so that for M2, $2\theta = 26.89^{\circ}$ (2Theta angle).

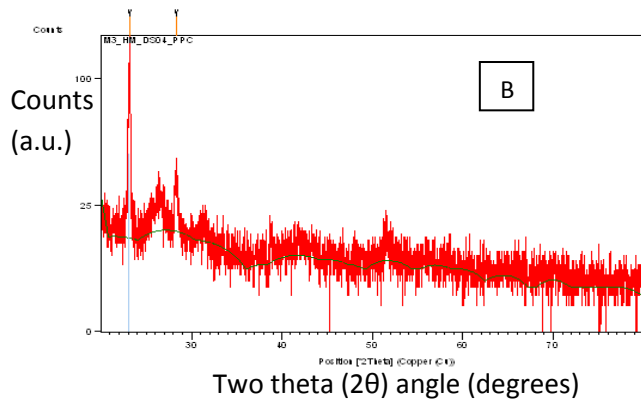
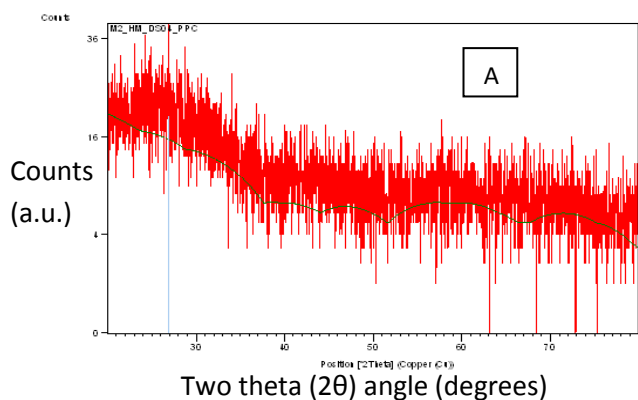


Fig. 3: XRD Patterns of Sulfated zirconia for sample M3

3.4 UV-VIS Spectrophotometry

The optical and solid state characterizations was done using spectrophotometric machine PYE-UNICAM UV-2102 PC in the ultra violet and visible regions for absorbance A, the transmittance T, refractive index, absorption coefficient and energy band gap of the film. The following results were obtained

3.4.1 Absorbance

The spectral absorbance of annealed sample at 573K is displayed in Fig.4. The result shows that the film samples absorb moderately at VIS regions but lowly in the UV regions. As such the maximum absorbance for the film occurred within the VIS region from where the absorbance decreased with the wavelength towards the UV region. At 1000nm wavelength, absorbance for the film samples M1, M2 and M3 measures 0.1, 0.2 and 0.3 respectively.

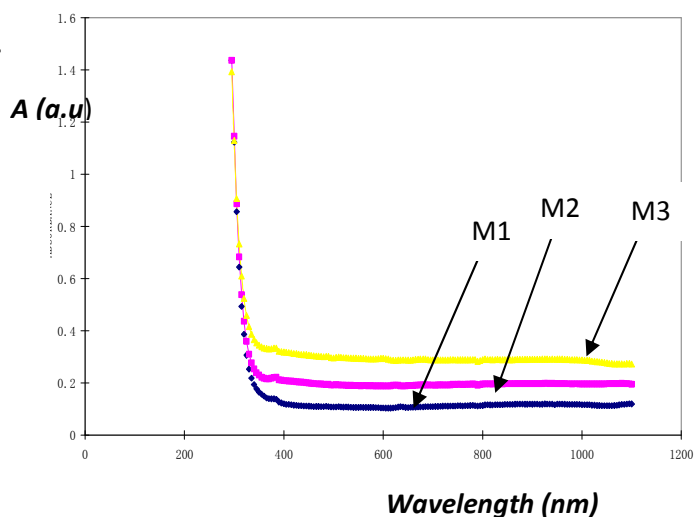


Fig. 4: Plot of absorbance as a function of wavelength (nm)

3.4.2 Transmittance:

The transmittance spectra (Fig. 5.) show that the film samples labeled M1, M2 and M3 have transmittance of about 76%, 64% and 51% at the wavelength of 1000nm respectively and transmittance of about 75%, 62% and 48% at the wavelength of 400nm respectively

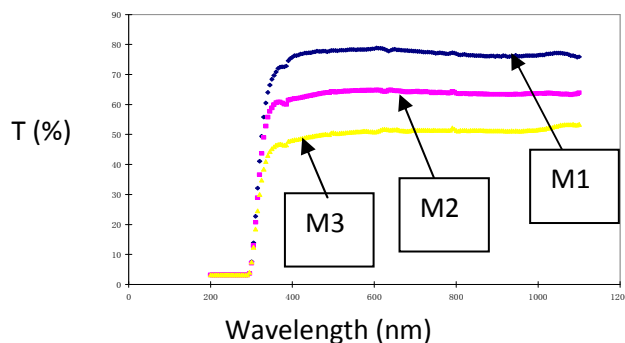


Fig. 5: Plot of transmittance (%) as a function of wavelength (nm)

3.4.3 Refractive Index:

The refractive index of sulphated zirconia (SZ) annealed at 573K (300°C) is displayed in Fig.6. The films samples show refractive index of approximately 1.63, 2.00 and 2.26 at photon energy of approximately 3.0eV for samples M1, M2 and M3 respectively.

3.4.4 Absorption coefficient

The absorption coefficient of sulphated zirconia (SZ) samples show an absorption coefficient of approximately 8.79, 15.54 and 23.73 at photon energy of approximately 3.0 eV for M1, M2 and M3 samples respectively.

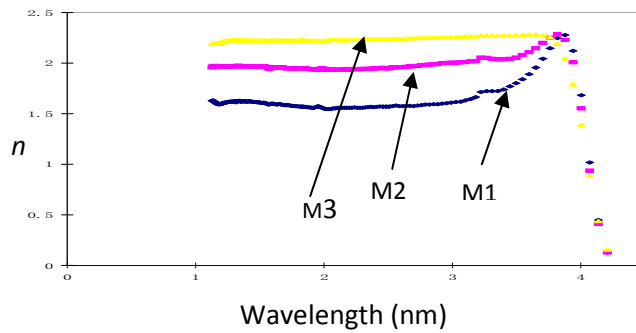


Fig. 6: Plot of refractive index as a function of photon energy (eV)

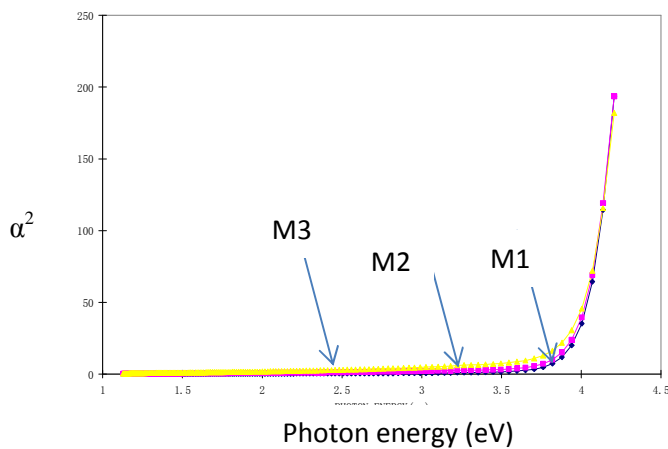


Fig. 7: Plot of absorption coefficient squared as a function of photon energy (eV)

4.4.5 Energy band gap:

Fig. 7 shows the energy band gap of sulphated zirconia (SZ) for the samples M1, M2 and M3. From the equation [22, 23],

$$(\alpha) = \left(\frac{A}{h\nu} \right) (h\nu - E_g)^n \quad (9)$$

where A is a constant, α is the absorption coefficient of the material, $h\nu$ is the incident radiation or photon energy of frequency ν and E_g is the bandgap of the material. The bandgap was estimated from the plot of α^2 versus photon energy (eV). The extrapolation of the straight line portion of the curve to zero of absorption coefficient (axis) gives the bandgap energy for direct bandgap materials. The estimated bandgap values are in the range of 3.80 to 4.00 ± 0.05 eV. For allowed direct bandgap materials, $n = 1/2$, and $n = 2$ for allowed indirect bandgap materials, $n = 3/2$ for forbidden indirect and $n = 3$ for forbidden indirect transitions. These values show that the material is a wide-bandgap material.

5. Conclusion

The sulfated zirconia (SZ) nanoparticles were successfully synthesized through chemical route, sol-gel and chemical bath technique. The structural, elemental, morphological and optical investigations were carried out on the materials by XRD, EDX, SEM and UV-VIS analysis. The samples deposited revealed that the film has a very high transmittance which decreases slowly with wavelength from UV to VIS regions. It also reveals that the film has low absorbance which increased slowly with wavelength from UV to NIR regions. Changes in concentration of the precursors affected the transmittance and absorbance of the film samples M1, M2 and M3. The result also shows that the energy band gap of sulfated zirconia lies within the range, 3.80 to 4.00 ± 0.05 eV. The film has high transmittance at almost all the regions but average absorbance at NIR region. This shows that it can be used in coating materials used in house hold mirror in which it will serve as a reflective interface. The high transmittance shows that it will be suitable for solar collectors to enhance solar energy collection. This will reduce the reflection of solar radiation and transmit radiation to the collector fluid and hence suitable for solar thermal applications.

Acknowledgment

The authors are grateful to the authorities of the University of Nigeria for providing us the professorial positions that made the research work possible and for the privilege of the use of the Crystal and Characterization Laboratory of the Department of Physics and Astronomy of the University.

References

- [1] Bansal, V., Rautaray, D., Ahmad, A. and Sastry, M., Biosynthesis of zirconia nanoparticles using the fungus *Fusarium oxysporum*. *J. Mater. Chem.*, Vol. 14, 2004, pp. 3303-3305.
- [2] Lovley, R., Stolz, J. F., Nord, G. L. and Phillips, E. J. F., Anaerobic production of magnetite by a dissimilatory iron-reducing microorganism. *Nature*, Vol. 330, 1987, pp. 252-254.
- [3] Jensen, D. G., Enhanced Toughness of a Partially Stabilised Zirconia at Elevated Temperatures, *Journal of the European Ceramic Society*, Vol. 16 (8), 1996, pp. 825-831.

- [4] Deville, S., Attaoui, H. E., Chevalier, Atomic force microscopy of transformation toughening in ceria-stabilized zirconia. *J. Journal of the European Ceramic Society*, Vol. 25, 2005. pp. 3089–3096.
- [5] Yang, H., Lu, R., Shen, L. C., Song, L. Z., Zhao, J. Z., Wang, Z. C., and Wang, L., Preparation, characterization and catalytic activity of sulfated zirconia-silica nanocrystalline catalysts. *Materials Letters*, Vol. 57, 2003, pp. 2572–2579.
- [6] Martins, R. L., and Schmal, M., Applied Catalysis A: General, Vol. 308, 2006, pp. 143–152.
- [7] Singh, B. P., Parchur A. K., Singh, R. K., Ansari, A. A., Singh, P. and Rai, S. B., Structural and up-conversion properties of Er^{3+} and Yb^{3+} co-doped $\text{Y}_2\text{Ti}_2\text{O}_7$ phosphors. *Phys. Chem. Chem. Phys.*, Vol. 15, 2013, pp. 3480–3489.
- [8] Somiya, S., Yamamoto, N., and Yanagina, H., 'Science and Technology of Zirconia III', in Advances in Ceramics, American Ceramic Society, Westerville, OH, Vols. 24A and 24B. 1988.
- [9] Heuer, A. H., Transformation Toughening in ZrO_2 -Containing Ceramics, *J. Am. Ceram. Soc.*, Vol. 70, 1987, p. 689.
- [10] Garvey, R. C., Hannic, R. H. and Pascoe, R. T., Ceramic steel, *Nature*, Vol. 258, 1975, p. 703.
- [11] Yamaguchi, T., Application of ZrO_2 as a catalyst and a catalyst support. *Catal. Today*, Vol. 20, 1994, pp. 199–218.
- [12] Chang-Bae Jeon, Seong-Ho Kong, and Jiyoung Kim, "Characteristics of zirconium silicate films prepared by using different co-sputtering methods", *Jour. Korean Physics Society*, Vol. 42, 2003, pp. 267–271.
- [13] Southon, P. D., Baotlett, J. R., Woolfrey, J. L. and Ben-Nissan, B., *Chem. Mater.*, Vol. 14, 2002, pp. 4313.
- [14] Raihani, H. A., Durand, B., Chassagneux, F., Kerridge, D. and Inman, D., *J. Mater. Sci.*, Vol. 4, 1994, p. 133.
- [15] Noh, H., Seo, D., Kim, H. and Lee, Synthesis and crystallization of anisotropic shaped ZrO_2 nanocrystalline powders by hydrothermal process J., *Mater. Lett.*, Vol. 57, 2003, pp. 2425–2431.
- [16] E. G. Gillan and R. B. Kaner, Rapid, energetic metathesis routes to crystalline metastable phases of zirconium and hafnium dioxide. *J. Mater. Chem.*, Vol. 11, 2001, pp. 1951–1956.
- [17] Yang, C., Hong, B., and Chen, J., Production of Ultrafine ZrO_2 and Y-Doped ZrO_2 Powders by Solvent Extraction from Solutions of Perchloric and Nitric Acid with Tri-n-Butyl Phosphate in Kerosene. *Powder Technol.*, Vol. 89, 1996, pp. 149–155.
- [18] Mazdiyasi, K.S., Lynchand, C.T., and Smith, J.S., Preparation of Ultra-High-Purity Submicron Refractory Oxides. *J. Am. Ceram. Soc.*, Vol. 48, 1965, pp. 372–375.
- [19] Adachi, M., Okuyama, K., Moon, S., Tohge, N., and Kousaka, Y., Preparation of Ultrafine Zirconium Dioxide Particles by Thermal Decomposition of Zirconium Alkoxide Vapour, *J. Mater. Sci.*, Vol. 24, 1989, pp. 2275–2280.
- [20] Fotou, G.P. Kodas, T.T., and Anderson, B., Coating Titania Aerosol Particles with ZrO_2 , $\text{Al}_2\text{O}_3/\text{ZrO}_2$, and $\text{SiO}_2/\text{ZrO}_2$ in a Gas-Phase Process *Aerosol Sci. Technol.*, Vol. 33, 2000, pp. 557–571.
- [21] Lenggoro, I.W., Hata, T., Iskandar, F., Lunden, M. M., and Okuyama, K., An Experimental and Modeling Investigation of Particle Production by Spray Pyrolysis Using a Laminar Flow Aerosol Reactor. *J. Mater. Res.*, Vol. 15, 2000, pp. 733–743.
- [22] Bhaskar, P. U., Babu, G. S., Kumar, Y.B. K, Jayasree, Y., Raja, V. S., Effect of bath concentration, temperature on the growth and properties of chemical bath deposited ZnS films, *Materials Chemistry and Physics*, Vol. 134, 2012, pp. 1106–1112.
- [23] Kassim, A., Ho, S. M., Abdullah, A.H. and Nagalingam, S., XRD, AFM and UV-Vis Optical Studies of PbSe Thin Films Produced by Chemical Bath Deposition Method, *Transactions C: Chemistry and Chemical Engineering*, Vol. 17, 2010, pp. 139–143.